DRX with Quick Sleeping: A Novel Mechanism for Energy Efficient IoT using LTE/LTE-A

Naveen Mysore Balasubramanya*, Lutz Lampe*, Gustav Vos† and Steve Bennett†
*Department of Electrical and Computer Engineering, University of British Columbia, Vancouver, Canada.
†Sierra Wireless Inc., Richmond, BC, Canada.

***Abstract*—The Third Generation Partnership Project (3GPP) has recognized Machine Type Communications (MTC) as a vital medium to drive the Internet of Things (IoT). One of the key challenges in MTC is to reduce the energy consumption of the MTC User Equipment (UE). Presently, the 3GPP Long Term Evolution (LTE)/LTE-Advanced (LTE-A) standards incorporate Discontinuous Reception (DRX) mechanism for this purpose. In this paper, we propose a modified DRX mechanism incorporating the Quick Sleeping Indication (QSI) as a novel, simple and energy efficient solution for low-complexity, low-mobility MTC UEs. We demonstrate our QSI transmission mechanisms using the broadcast and synchronization channels of LTE/LTE-A for MTC UEs in normal coverage and using the data channel for MTC UEs operating in "coverage enhancement" (CE) mode. For MTC UEs in normal coverage, our simulation results and analysis show that our DRX with QSI mechanisms result in 45% improvement in the energy efficiency and 66% reduction in the computational complexity at the UE receiver, when compared to the current DRX mechanism. For MTC UEs with CE, the energy and computational efficiency increase to 63% and 68% respectively.**

***Index Terms*—Long Term Evolution (LTE), LTE-Advanced (LTE-A), Machine Type Communications (MTC), Internet of Things (IoT), Discontinuous Reception (DRX), Paging, Quick Sleeping Indication (QSI).**

I. Introduction

THE Internet is progressing from connecting dedicated terminals to providing a common platform to connect various devices like tablets, smart phones, location sensors, smart meters, etc. This enticing aspect of realizing the Internet of Things (IoT) has actuated numerous challenges spread across different fields of research. One of the key challenges for IoT is to determine efficient mechanisms to connect these devices.

Various physical and link layer technologies are being considered to serve the IoT devices. The prominent solutions include IEEE 802.15.4 Bluetooth [1], [2], IEEE 802.11 Low Power Wireless Local Area Network (WLAN) [3], [4], which mainly rely on device-to-device (D2D) communication and a distributed network architecture. However, these technologies are limited by low coverage and capacity. Recently, heterogeneous networks and small cell base-stations [5], [6] are being deployed to serve regions where the network traffic is high. Although these solutions are successful in managing the network load and improving the user throughput, the additional infrastructure and operational expenses required to realize these solutions are high. IoT solutions also include self organizing networks (SONs), which have the ability to improve the network efficiency by adapting, managing and optimizing their operations based on the network behaviour [7], [8]. However, SONs require complex algorithms and new network equipment to operate efficiently.

Another promising solution for IoT is the Machine Type Communications (MTC). It serves as a facilitator for IoT by defining the communication and service mechanisms to connect the various devices. MTC devices need to serve diverse IoT applications ranging from intelligent transportation, smart grids and healthcare to location sensors and pet trackers [9]. MTC faces the challenge of handling this application diversity effectively. Moreover, various services corresponding to these applications are conceptualized to be over the cellular network. For example, services like smart metering for utilities, security monitoring and reporting use the cellular network for communication. With the IoT services emerging as the constitutive driver for the growth of cellular network and MTC assisting the communication mechanisms, the 3rd Generation Partnership Project (3GPP) has initiated the standardization of MTC from Release 11 of the Long Term Evolution (LTE) standard. The major advantages of using MTC over the LTE network for IoT are that it uses the existing network infrastructure to serve the devices, thereby reducing the operational costs and it enables the network operator to harness the higher capacity, coverage and ease of integration aspects of LTE to serve the devices efficiently.

Since the MTC devices are application specific, the Quality of Service (QoS) requirements of MTC devices are also varied. While human operated devices like smartphones can be delay sensitive, possess high mobility and demand high data rates, MTC devices used for sensing such as smart meters and pet trackers have low mobility, access the network infrequently and are more delay tolerant, thereby demanding communication mechanisms that can handle low data rates effectively. The 3GPP has identified such MTC devices as Category-0 (CAT-0) devices which can support a maximum data rate of 1Mbps [10], [11]. MTC devices can be placed in locations like the interior of buildings, underground parking lots and basements where the network coverage is low. For example, MTC devices can be used for medical monitoring where vital biological parameters of patients such as blood pressure, heart rate and body temperature are sensed and exchanged with a server [12]. The patients have limited mobility within the hospital premises and can be present in a closed, indoor environment where the network requires enhanced coverage to reach them. The 3GPP has also identified MTC UE operation with coverage

enhancement (CE) as a "work item" in Release 13 aiming to provide 12dB to 20dB of additional coverage [10], [11]. Additionally, the MTC network has to manage a large number of devices though efficient usage of network resources and available power.

The network architecture of LTE/LTE-Advanced (LTE-A) needs to be enhanced to support MTC applications [13], [14] and energy efficiency is one of the key aspects to be addressed in the design of new MTC mechanisms [15]. The current LTE/LTE-A standards use Discontinuous Reception (DRX) to reduce the power consumption of the User Equipment (UE) during which the UE follows a sleep and wake-up cycle [16]–[19]. The UE wakes up periodically to check for paging information from the base-station (eNB).

The analysis of the DRX mechanism and the resulting power consumption have been studied in many previous works. In [20], the DRX mechanism is modelled for bursty packet data traffic using a Semi-Markov process. In [21], the authors have provided a numerical analysis of the DRX by dividing the DRX operation into several independent parts and combining the result obtained from each part. In [22], a Semi-Markov chain model is developed to analyze the DRX mechanism for MTC applications, which can be used to estimate the choice of DRX parameters. A model to analyze the latency incurred by the DRX mechanism for active and background mobile traffic is developed in [23]. Recently, an in-depth analysis of the average delay and power consumption of the DRX mode using recursive deduction and Markov models is provided in [24]. Also, in [25] and [26], it is shown that extending the length of the DRX cycle helps in reducing the energy consumption of the UE. However, these works address the DRX operation for UEs in normal coverage and assume perfect timing synchronization. For the low-cost, low-complexity CE MTC UEs, the authors in [27] demonstrate a new mechanism where the UE does not check for the page periodically and turns ON its radio only for data transmission, thereby reducing the energy consumption of the UE. However, this mechanism is applicable to transmit driven UEs and cannot be used by UEs which require timely information from the eNB to operate successfully.

Though the DRX procedure results in significant power reduction, the amount of power spent by the UE during the wake-up time or the ON time is still considerable since the decoding of paging information is computationally intensive. Also, the UE may need to re-acquire timing synchronization due to the drift in the UE clock which further increases the ON time. Moreover, in the IoT scenario, due to the presence of a huge number of devices, the probability of the UE receiving a page during each ON period is substantially low. However, the UE still looks for paging information every time it wakes up and expends a significant amount of power. Therefore, we propose the Quick Sleeping Indication (QSI) mechanism to indicate to the UE whether it can sleep early since there is no valid incoming page [28]. When our QSI mechanism is used, the UE would first decode the QSI message and if it indicates "sleep", the UE goes back to sleep immediately. If the QSI indicates "stay-awake", the UE remains ON for decoding the subsequent paging block. It would be helpful to the UE if the QSI mechanism is simple and structured such that the UE can decode it with low complexity and reduced power consumption.

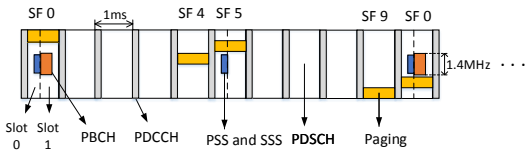

Fig. 1. Frame structure in LTE/LTE-A.

In this paper, we provide the QSI design mechanisms for energy efficient IoT using LTE/LTE-A. We consider two categories of MTC UEs - a) without CE and b) with CE. Our QSI mechanisms are not only simple to implement, but also require minimal changes to the present 3GPP LTE/LTE-A standardization framework. We show that we can obtain substantial improvement in energy efficiency and significant reduction in computational complexity using our novel QSI mechanisms for MTC UEs with and without CE.

The rest of the paper is outlined as follows. In Section II, we explain the DRX and paging mechanism adopted in the current 3GPP LTE/LTE-A standard and introduce our DRX and paging with QSI mechanism. In Section III, we discuss the QSI mechanisms for MTC UEs without CE. In Section IV, we consider the case of MTC UEs with CE and demonstrate our QSI mechanisms for this case. We follow up with the energy efficiency and computational complexity analysis in Section V and the simulation results in Section VI. We conclude our work in Section VII.

II. DRX, Paging and Quick Sleeping Mechanisms

The UEs operating using the 3GPP LTE/LTE-A standard use the DRX mechanism in order to save power. In the DRX mode of operation, the UE has to wake up periodically to check for a paging message [16]. The longest DRX cycle supported in the present LTE/LTE-A standard is 2.56s, but extended length DRX cycles are being proposed for MTC UEs to enable further power reduction [10], [11]. In this section, we explain the present paging mechanism for UE and the different DRX modes supported in LTE/LTE-A. Then, we propose our modified DRX mechanism with quick sleeping for energy efficient DRX.

A. Current paging reception mechanism for UE in DRX

The control information for an upcoming paging block is indicated to the UE by a Physical Downlink Control Channel (PDCCH) containing the Paging-Radio Network Temporary Identifier (P-RNTI) followed by the paging data on the Physical Downlink Shared Data Channel (PDSCH). The paging data consists of a list of the System Architecture Evolution-Temporary Mobile Subscriber Identity (S-TMSI) or the International Mobile Equipment Identity (IMEI) of the UEs being paged. If the UE successfully decodes a PDCCH with P-RNTI and the paging block on PDSCH and finds its S-TMSI or IMEI in the paging list, then it stays awake to decode an impending data transmission. Otherwise, it goes back to sleep. For decoding the PDCCH, the UE requires

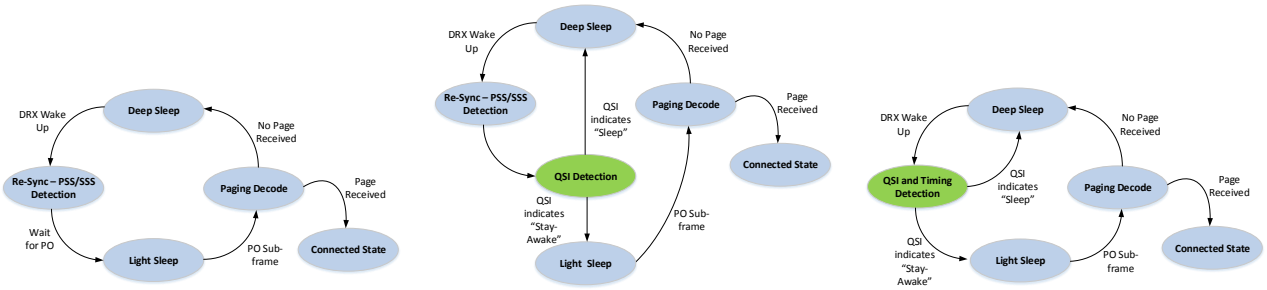

(a) Current DRX model in LTE/LTE-A (b) Proposed DRX model with QSI (without CE) (c) Proposed DRX model with QSI (with CE)

Fig. 2. Current and proposed DRX Models.

a Fast Fourier Transform (FFT) whose size corresponds to the eNB bandwidth and incorporates a blind decoding scheme where it hypothesizes over 44 options of PDCCH locations [18], [29]. This renders the PDCCH decoding procedure to be computationally intensive and power consuming.

B. DRX Modes supported in LTE/LTE-A

The LTE/LTE-A standard supports two variants of DRX - a) Connected Mode DRX and b) Idle Mode DRX [17]–[19]. These modes are categorized based on the handling of the Radio Resource Configuration (RRC) connection. In the Connected Mode DRX, the UE does not relinquish the RRC connection for the entire duration of the DRX cycle and in the Idle Mode DRX, the UE releases the RRC connection before it goes back to sleep. In this work, we focus on the Idle Mode DRX mechanism since the Connected Mode DRX is relevant to devices like smartphones which require frequent network access. The Idle Mode DRX is applicable to low-data rate MTC UEs, which form an integral part of IoT, that are delay tolerant and access the network infrequently.

In the Idle Mode DRX, each UE checks for PDCCH periodically, albeit only in one pre-assigned sub-frame per DRX cycle called the Paging Occasion (PO) [19]. The PO sub-frame number is determined based on the UE Identifier (UEID) and it can be either sub-frame 0, 4, 5 or 9 as shown in Fig. 1. This can ideally reduce the ON time of the UE to just 1ms if the Signal-to-Noise Ratio (SNR) is good and the timing synchronization of the UE is so accurate that it can wake up exactly at the PO. However in practice, the Voltage Controlled Crystal Oscillator (VCO) used for the UE clock will possess a drift that can affect the symbol timing accuracy and SNR may not always be favourable. If the sub-frame timing is not accurate, the UE will have to re-acquire it using the Primary Synchronization Signal (PSS) and the Secondary Synchronization Signal (SSS). Similarly, if the frame timing is lost, the UE will have to re-acquire frame synchronization by decoding the system frame number (SFN) transmitted on the Physical Broadcast Channel (PBCH) [29].

Fig. 2a shows the different states traversed by a legacy UE implementing the present Idle Mode DRX mechanism. The UE is initially in a "Deep Sleep" state where only the UE clock is active and all other processing units including the radio are OFF. At the wake up time instant, the UE wakes up from DRX and resynchronizes with the eNB by detecting PSS/SSS and PBCH (if the UE timing has drifted more than half a sub-frame). After synchronization, the UE transitions to a "Light Sleep" state where only the clock, radio and channel estimation blocks are ON and the Tx/Rx processing blocks are OFF. The duration of light sleep depends on the PO. If the PO corresponds to the PSS/SSS sub-frame (i.e. on sub-frame 0 or 5), the UE proceeds to the "Paging Decode" state immediately (see Fig. 1). But if the PO is on sub-frame 4 or 9, the UE waits for the PO by moving to the "Light Sleep" state and it transitions to "Paging Decode" state on the PO sub-frame. In the "Paging Decode" state, the UE decodes the PDCCH and the PDSCH (if the PDCCH contains the P-RNTI) for the paging information and moves to the "Connected State" if there is a valid page. Otherwise, it goes back to the "Deep Sleep" state[1].

C. DRX and Paging with QSI

The energy consumed by the UE for checking for a page can be segregated into two categories - a) energy consumed by the UE radio during its ON time for paging decoding and b) energy consumed by the UE baseband processing unit for the computationally intensive paging decode operation. It would be convenient to have a procedure through which the UE can quickly obtain the information about an upcoming page and go back to sleep immediately when there is no page since this would reduce the ON time of the UE and the corresponding energy consumed. If this procedure is designed such that the UE can determine the paging information in baseband using low complexity techniques, it would also save energy by being computationally efficient. In this paper, we introduce the DRX and paging with quick sleeping as the solution for energy efficient operation of MTC UEs using LTE/LTE-A.

Since the number of MTC UEs for IoT might be large, we propose to divide the UEs into multiple groups and assign M bits for the QSI message which would put one or more UE groups to sleep when there is no impending page for the group. The network has the flexibility to configure the manner in which the QSI addresses the UE groups. One configuration that the network can use is a bit-map addressing mode where one bit is assigned exclusively to one UE group and the

[1]The "Light Sleep" and "Deep Sleep" terminology is conventionally used for Short DRX and Long DRX respectively [20]. In the context of this work, they are used somewhat differently and indicate the sleep status of the UE.

network can address up to M groups. For example, with $M = 4$, we can address 4 UE groups and the QSI message "1010" indicates that the UE groups 1 and 3 can be put to sleep.

Fig. 2b demonstrates our first model for DRX and paging with QSI which we use for MTC UEs without CE. In this model, the UE begins its paging detection operation similar to the legacy UE, by transitioning from the "Deep Sleep" state to the "Re-sync State" to acquire the symbol boundary when it wakes up from the DRX cycle. However, after the timing acquisition, the UE transitions to the "QSI Detection" state where it detects the QSI signal. If the QSI conveys "sleep" since there is no valid upcoming page, then the UE immediately transitions into the "Deep Sleep" state. However, if the QSI signals indicates "stay-awake" or if the QSI is not detected successfully, the UE resumes the legacy operation for decoding the paging information and transitions to the "Light Sleep" state.

The MTC UEs can be deployed in places like interiors of buildings and basements where the network coverage is low. When the SNR is low, multiple PSS/SSS copies will have to be combined for successful detection and timing synchronization. The PSS/SSS is transmitted every 5ms and the UE has to stay ON longer if it requires multiple copies of PSS/SSS. Also, the PDCCH and PDSCH decoding might require multiple repetitions to be decoded successfully which would further increase the ON time and the computational complexity for paging decode. Therefore, it is beneficial to have a QSI signal which can also be used for sub-frame synchronization for MTC UEs with CE. In this case, the different combinations of M QSI bits are mapped to different sequences, thereby resulting in 2^M QSI sequences. The sequence corresponding to the QSI message is transmitted periodically. The UE receiver detects the transmitted QSI sequence by hypothesizing over the set of 2^M QSI sequences and decodes the QSI message as well as the timing information. Fig. 2c depicts our second model for DRX and paging with QSI for CE. The UE begins its paging detection operation by transitioning from the "Deep Sleep" state to the "QSI and Timing Detection" state where it jointly obtains the timing and sleeping indication. If the QSI conveys "sleep", the UE moves back to the "Deep Sleep" state immediately and if the QSI indicates "stay-awake", the UE transitions to the "Light Sleep" state and decodes the page by moving to the "Paging Decode" state on the PO. If the QSI is not detected, then the UE follows legacy DRX operation in order to decode the paging information.

In the following, we present different implementations for the proposed DRX and paging with QSI for MTC UEs without CE and with CE. Our QSI solutions are designed such that they are compatible with the LTE/LTE-A framework and help in energy efficient operation of MTC UEs for IoT.

III. Quick sleeping solutions for MTC UEs without CE

In this section, we discuss the QSI mechanisms for MTC UEs without CE. This is applicable to the IoT scenario of pet tracking or weather sensing in which the UEs have low-mobility and are located in regions where the network coverage is good. In this case, we design the QSI such that it reuses the resources that are already being allocated by the eNB. We choose to transmit the QSI on those physical channels whose locations on the sub-frame grid do not change so that the UE is aware of the location of the QSI. The physical channels for synchronization and broadcast comply with our requirement since they invariably occupy the centre 6 Resource Blocks (RBs) [29]. In particular, the SSS and PSS are always transmitted on the last two symbols of the first slot of sub-frame 0 and sub-frame 5 and the PBCH is always transmitted on the first 4 symbols of the second slot of sub-frame 0 (see Fig. 1). Hence, in the following we describe simple and efficient techniques to transmit QSI on PBCH and PSS/SSS.

A. QSI on PBCH

The PBCH is sent on sub-frame 0 of each radio frame. Therefore, it is transmitted every 10ms and each 10ms block will contain 240 out of the 960 complex Quadrature Phase Shift Keying (QPSK) symbols [29]. We advocate for the following solutions for QSI on PBCH first introduced in our conference paper [28].

1) Spreading QSI using repetition only: In this mechanism, we spread the M QSI bits over the original 10ms PBCH signal which consists of 480 bits (240 QPSK symbols). Then, the QSI vector is modulated using QPSK, multiplied by a phase randomizing sequence (RS) to ensure a uniform phase distribution and added to the original 10ms PBCH signal at a very low power. The SNR of the QSI signal is given by $\mathrm{SNR_p} = \frac{S_\mathrm{p}}{N_0}$ where S_p and N_0 denote the QSI signal power and noise power respectively. Considering that, P, a fraction of the PBCH transmission power is being used for QSI transmission, the effective SNR of QSI due to spreading is $P \cdot \mathrm{SNR_p} \cdot SPF$ where the spreading factor $SPF = \frac{480}{M}$. The QSI bits can be detected after subtracting the original PBCH signal from the received signal since the spreading gain increases the effective SNR of the QSI signal. The expected loss in PBCH detection performance is derived as $\frac{(1-P)}{(P \cdot SNR_p + 1)}$.

2) Spreading QSI using repetition and forward error correction (FEC): In this method, we encode the M QSI message bits to get M_enc encoded QSI bits and spread these bits over the 480 PBCH bits using repetition. The resulting spreading factor is $SPF = \frac{480}{M_\mathrm{enc}}$. The QSI signal is decoded after subtracting the original PBCH signal and the SNR of the QSI signal is diminished by a factor of $\frac{M}{M_\mathrm{enc}}$ compared to the solution in Section III-A1. However, the gain from FEC compensates for the reduction in SNR. Moreover, when M is not to large, the number of QSI sequences (2^M) will be relatively small and a simple Maximum Likelihood (ML) decoding scheme can be used for FEC decoding.

B. QSI on PSS/SSS

PSS and SSS are the synchronization signals used in LTE/LTE-A transmitted on the centre band. The PSS is a 63-length Zadoff-Chu (ZC) sequence which is sent with a

TABLE I
QSI TRANSMISSION METHODS USING UNUSED SUB-CARRIERS ON PSS AND SSS

Method	C_{m}	FEC Used	N_{s}	N_{r}
1	BPSK	No	1	2
2	BPSK	No	2	4
3	BPSK	Yes	1	1
4	BPSK	Yes	2	2

periodicity of 5ms on the last symbol of the first slot in sub-frame 0 and sub-frame 5. The 32^{nd} carrier corresponds to the DC sub-carrier and it is set to zero [29]. The SSS consists of two 31-length m-sequences on either side of the DC sub-carrier. The SSS is also sent in sub-frame 0 and sub-frame 5 one symbol before the PSS. But the SSS on sub-frame 0 is not the same as the one on sub-frame 5 and this helps the UE determine if it is on the first half of the radio frame or the second half during acquisition [29]. The centre band spanning 1.4MHz consists of 72 sub-carriers including the DC sub-carrier. The key feature of both PSS and SSS transmissions is that they use only 62 out of the 72 sub-carriers. Thus, excluding the DC carrier, we still have 9 unused sub-carriers. We therefore propose to transmit M QSI bits using 8 out of the 9 unused sub-carriers.

For this mechanism, we consider the case where $M \leq 4$ and build a 4-bit QSI message. When $M \leq 2$, the bits can be repeated and when $M = 3$, a zero can be appended as the Most Significant Bit (MSB) in order to obtain the 4-bit QSI message. Let C_{m} and N_{s} denote the modulation scheme and the number of synchronization symbols used for QSI transmission respectively. The number of repetitions required to accommodate the 4-bit message on the unused sub-carriers is $N_{\mathrm{r}} = \frac{8 \cdot N_{\mathrm{s}}}{4} = 2N_{\mathrm{s}}$. Table I summarizes variants for the proposed QSI transmission on PSS/SSS using different repetition factors without and with FEC. For the latter, we suggest a (8,4) Extended Hamming Code, because we use 8 unused sub-carriers per synchronization symbol to accommodate the 4-bit QSI message.

We assume that the eNB has to use a part of the available power for transmitting the QSI. When there is no QSI, the eNB transmission power is uniformly distributed over 62 sub-carriers and in the presence of QSI, it is distributed uniformly over 70 sub-carriers. Therefore, the loss in PSS/SSS SNR when QSI is transmitted can be computed as $10\log_{10}(\frac{62}{70}) = -0.53$dB, which is a small degradation from the original value. If the eNB can afford additional power for QSI transmission, there will be no degradation in PSS/SSS performance.

IV. Quick Sleeping Solution for MTC UEs with CE

In the case of IoT, the UEs may be located in places like underground parking lots to sense vacant parking spots or in the interior of buildings such as hospitals to monitor the status of the patients where the network coverage is very low. The solutions discussed in Section III do not work effectively in this case, because the UE will need multiple repetitions of PSS/SSS to determine the timing since the SNR is very low. And if the UE needs to re-acquire PBCH, it would need multiple copies of PBCH to accurately determine the SFN. Similarly, decoding the paging on PDCCH, PDSCH and the QSI will also require multiple repetitions, which increases the ON time of the UE. Therefore, it is preferable to design a robust QSI signal which not only indicates whether a group of UEs can be put to sleep quickly, but also helps in faster timing synchronization. A UE decoding such a QSI signal would obtain both the paging and timing information in parallel which could reduce the ON time and paging decoding complexity, thereby saving energy. In this section, we present the QSI signal design mechanism for MTC UEs with CE using dedicated resources in the PDSCH space.

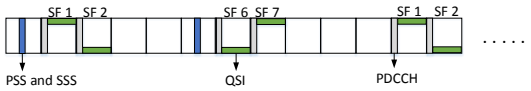

Fig. 3. QSI transmission mechanism on PDSCH.

In particular, we propose to use ZC sequences to create QSI signals which possess good auto-correlation and cross-correlation properties and thus enable robust signal detection. ZC sequences are Constant-Amplitude-Zero-Auto-Correlation (CAZAC) sequences and cyclically shifted versions of these sequences are orthogonal to each other [29]. Also, the cross-correlation of two ZC sequences of length N is limited by $\frac{1}{\sqrt{N}}$. They are already being used in LTE/LTE-A for PSS and random access. The proposed QSI ZC sequence is of the form

$$\mathrm{QSI}_{\mathrm{ZC}}(p) = \mathrm{e}^{\left(\frac{-j\pi pn(n+1)}{N}\right)} \tag{1}$$

where, $N = 131$ is the length of the ZC sequence and p is the root of the ZC sequence chosen such that it is co-prime with N. We choose $p \in [2 + 8 \cdot (q-1)]$ where $q = 1, 2, \cdots 16$. The QSI sequence occupies 131 sub-carriers or Resource Elements (REs). This length is chosen because a legacy paging block would take at least 1 Physical Resource Block (PRB) and considering 2 symbol-PDCCH, this would occupy 132 REs [17], [18]. One could always choose a longer length sequence to improve the performance since the cross-correlation peak is inversely proportional to the length of the sequence,but a longer sequence would require more resources.

Our proposed QSI transmission mechanism in the PDSCH space uses 1 PRB in sub-frames 1, 2, 6 and 7 of a radio frame. These sub-frames are chosen to provide time diversity to the QSI signal and ensure that it is periodic. We use the centre 1.4MHz band and transmit the QSI ZC sequence on the top PRB of sub-frames 1 and 7 and the bottom PRB of sub-frames 2 and 5, thereby introducing some frequency diversity to the QSI signal. This also ensures that the QSI pattern has a periodicity of 10ms and the UE can determine the exact sub-frame number when it detects the QSI. Fig. 3 illustrates the proposed QSI signaling pattern.

V. Energy Consumption and Computational Complexity Analysis

In this section, we analyze the reduction in UE energy consumption and the number of UE computations for our different QSI solutions. Prior to this work, the energy consumption of the UE in DRX mode has been analyzed using a Semi-Markov

chain model [20], [22] or a queueing based model [21]. In our work, we use a simpler model where the energy consumption is derived from the ON time of the UE similar to [25] and the computational complexity is determined using the number of FFT operations performed by the UE.

A. Energy consumption analysis

Let t_{DRX}, t_{Sync} and t_{Paging} denote the total time of UE DRX cycle, time taken by the UE for synchronization and the UE ON time for paging decode respectively. The time spent by the UE in the "Light Sleep" state and the drift time of the UE clock are represented by t_{LS} and t_{Drift} respectively. P_{ON}, P_{LS} and P_{DS} denote the power consumed by the UE during the ON state, the "Light Sleep" state and the "Deep Sleep" state respectively.

1) Legacy UE in Idle Mode DRX: Firstly, we consider the case of a legacy UE without CE at an operating SNR good enough to decode PSS/SSS and PBCH in the first attempt. For PSS/SSS detection, we assume that the UE is ON for a duration one sub-frame since the UE has to search for PSS/SSS within the buffered sub-frame which gives $t_{\mathrm{Sync}} = 1$ms. When the paging sub-frame is 0 or 5, the legacy UE does not wait for PO and $t_{\mathrm{LS}} = 0$. However, if the paging sub-frame is 4 or 9, the UE decodes the PSS/SSS on sub-frame 0 or on sub-frame 5 and has to wait 3 more sub-frames for its PO. The UE goes into "Light Sleep" for these sub-frames, which gives $t_{\mathrm{LS}} = 3$ms. In the case of MTC for IoT, due to the large number of UEs being paged, we can assume that the POs are equally likely and compute the average light sleep time $t_{\mathrm{LS}}^{\mathrm{avg}} = \frac{0+3+0+3}{4} = 1.25$ms. The total ON time of the legacy UE is given by $t_{\mathrm{ON}}^{\mathrm{Legacy}} = t_{\mathrm{Drift}} + t_{\mathrm{Sync}} + t_{\mathrm{Paging}}$. Therefore, the energy consumed by the legacy UE can be calculated as

$$E_{\mathrm{Legacy}} = t_{\mathrm{ON}}^{\mathrm{Legacy}} P_{\mathrm{ON}} + t_{\mathrm{LS}}^{\mathrm{avg}} P_{\mathrm{LS}} + (t_{\mathrm{DRX}} - t_{\mathrm{ON}}^{\mathrm{Legacy}} - t_{\mathrm{LS}}^{\mathrm{avg}}) P_{\mathrm{DS}}. \quad (2)$$

Secondly, we consider the case of a legacy UE with CE. In this case, the SNR is low and multiple repetitions are required for successful detection of PSS/SSS and paging. Therefore, the total energy consumed by the legacy UE with CE can be calculated using (2) with $t_{\mathrm{ON}}^{\mathrm{Legacy}} = t_{\mathrm{Drift}} + t_{\mathrm{Sync}}^{\mathrm{CE}} + t_{\mathrm{Paging}}^{\mathrm{CE}}$ where $t_{\mathrm{Sync}}^{\mathrm{CE}}$ and $t_{\mathrm{Paging}}^{\mathrm{CE}}$ denote the ON time required for PSS/SSS detection and paging decode with CE respectively.

2) MTC UE without CE adopting our DRX with QSI mechanism: Here, the QSI is transmitted on PBCH or on PSS/SSS. In both the cases, similar to the legacy case, $t_{\mathrm{Sync}} = 1$ms, but the average light sleep time varies depending on where the QSI is transmitted and whether PBCH decoding is necessary. If the QSI is transmitted on PSS/SSS and PBCH decoding is not necessary, then the average light sleep time is the same as that of the legacy UE, that is, $t_{\mathrm{LS}}^{\mathrm{avg}} = 1.25$ms. However, if the QSI is transmitted on PBCH or if the UE has slept long enough so that PBCH decoding is necessary, then the UE wakes up at sub-frame 0 regardless of the PO, detects PSS/SSS on sub-frame 0, decodes the PBCH, obtains the QSI and goes into "Light Sleep" until the PO sub-frame. Therefore, t_{LS} can be 0ms, 3ms, 4ms or 8ms and the average light sleep time $t_{\mathrm{LS}}^{\mathrm{avg}} = 3.5$ms. Let p indicate the probability of successful QSI detection and q indicate the probability that the QSI conveys "sleep". Then, the probability of successful QSI detection and UE going back to sleep is pq and the total ON time for the UE in this case will be $t_{\mathrm{QSI}} = t_{\mathrm{Drift}} + t_{\mathrm{Sync}}$. The corresponding energy consumed by the UE is

$$E_1 = t_{\mathrm{QSI}} P_{\mathrm{ON}} + (t_{\mathrm{DRX}} - t_{\mathrm{QSI}}) P_{\mathrm{DS}}. \quad (3)$$

If the QSI is detected successfully and the UE has to stay awake for paging or if the QSI signal is not detected, the UE resumes legacy mode of operation. This occurs with probability $(1 - pq)$ and the energy consumed by the UE is E_{Legacy} given by (2). Therefore, the total energy consumption of the UE without CE adopting QSI can be calculated as

$$E_{\mathrm{QSI}} = pqE_1 + (1 - pq)E_{\mathrm{Legacy}}. \quad (4)$$

3) MTC UE with CE adopting our DRX with QSI mechanism: In this case, the UE attempts to decode the QSI transmitted on PDSCH which gives the UE both the timing information as well as sleeping indication. The QSI signal detection, PSS/SSS detection and paging decode operations will take t_{Q}, $t_{\mathrm{Sync}}^{\mathrm{CE}}$ and $t_{\mathrm{Paging}}^{\mathrm{CE}}$ amount of time respectively since the SNR is low and multiple repetitions are required for successful detection. The UE has to wake up at least t_{Q} + $t_{\mathrm{Sync}}^{\mathrm{CE}}$ before the PO since it has to first detect QSI and if it fails, the UE should fall back to legacy operation, detect PSS/SSS followed by paging decode. The ON time for QSI detection will be $t_{\mathrm{QSI}}^{\mathrm{CE}} = t_{\mathrm{Drift}} + t_{\mathrm{Q}}$. The energy consumed by the UE if it detects QSI successfully and the QSI indicates "sleep" (which occurs with probability pq) is given by

$$E_1^{\mathrm{CE}} = t_{\mathrm{QSI}}^{\mathrm{CE}} P_{\mathrm{ON}} + (t_{\mathrm{DRX}} - t_{\mathrm{QSI}}^{\mathrm{CE}}) P_{\mathrm{DS}}. \quad (5)$$

If the QSI is detected successfully and it indicates "stay-awake", the UE goes into the "Light Sleep" state until the PO sub-frame and then decodes the paging on the PO sub-frame. This occurs with probability $p(1 - q)$ and the energy consumed by the UE is

$$E_2^{\mathrm{CE}} = (t_{\mathrm{QSI}}^{\mathrm{CE}} + t_{\mathrm{Paging}}^{\mathrm{CE}}) P_{\mathrm{ON}} + (t_{\mathrm{Sync}}^{\mathrm{CE}} + t_{\mathrm{LS}}^{\mathrm{avg}}) P_{\mathrm{LS}} + (t_{\mathrm{DRX}} - t_{\mathrm{QSI}}^{\mathrm{CE}} - t_{\mathrm{Paging}}^{\mathrm{CE}} - t_{\mathrm{Sync}}^{\mathrm{CE}} - t_{\mathrm{LS}}^{\mathrm{avg}}) P_{\mathrm{DS}}. \quad (6)$$

If the UE is unable to detect the QSI signal, then it resumes legacy operation and this scenario occurs with probability $(1 - p)$. The energy consumed is

$$E_3^{\mathrm{CE}} = (t_{\mathrm{QSI}}^{\mathrm{CE}} + t_{\mathrm{Sync}}^{\mathrm{CE}} + t_{\mathrm{Paging}}^{\mathrm{CE}}) P_{\mathrm{ON}} + t_{\mathrm{LS}}^{\mathrm{avg}} P_{\mathrm{LS}} + (t_{\mathrm{DRX}} - t_{\mathrm{QSI}}^{\mathrm{CE}} - t_{\mathrm{Sync}}^{\mathrm{CE}} - t_{\mathrm{Paging}}^{\mathrm{CE}} - t_{\mathrm{LS}}^{\mathrm{avg}}) P_{\mathrm{DS}}. \quad (7)$$

Therefore, the total energy consumption of the UE adopting QSI can be calculated as

$$E_{\mathrm{QSI}}^{\mathrm{CE}} = pqE_1^{\mathrm{CE}} + p(1 - q)E_2^{\mathrm{CE}} + (1 - p)E_3^{\mathrm{CE}}. \quad (8)$$

B. Computational complexity analysis

The paging decoding requires PDCCH decoding as its first step regardless of whether the UE is being paged or not. PDCCH requires a full eNB bandwidth size FFT which requires $O(N \log_2 N)$ computations, N being the FFT size.

1) Legacy UE in Idle Mode DRX: First, we consider the case of a legacy UE without CE which takes one sub-frame

for PSS/SSS detection to re-acquire the timing and one sub-frame to decode the paging block. The PSS/SSS and the PBCH require a 128 point FFT [29]. Considering that for normal length cyclic prefix (CP), we have 14 symbols in a sub-frame, the number of FFT operations for synchronization is $n_{\text{Sync}} = 14 \times 128 \log_2(128) = 12544$. Assuming that the PDCCH occupies m symbols, the UE would require $n_{\text{PDCCH}} = m \cdot O(N \log_2 N)$ operations for PDCCH FFT. If the PDCCH indicates P-RNTI, the UE has to proceed to decode the PDSCH which will add to the number of FFT operations of the UE. For this analysis, we take into account only the synchronization and PDCCH FFT operations for the legacy UE since we model the scenario where a UE is very rarely paged and the contribution of PDSCH FFT to the total number of FFT operations is not significant. The total number of FFT operations for the legacy UE is computed as

$$n_{\text{Legacy}} = n_{\text{Sync}} + n_{\text{PDCCH}}. \tag{9}$$

For the legacy UE with CE, the total number of FFT operations will be

$$n^{\text{CE}}_{\text{Legacy}} = n_{\text{Sync}} r_{\text{Sync}} + n_{\text{PDCCH}} r_{\text{PDCCH}}. \tag{10}$$

where r_{Sync} and r_{PDCCH} is the number of PSS/SSS and PDCCH repetitions required for successful decoding respectively.

2) MTC UE without CE adopting our DRX with QSI mechanism: Here, the QSI is sent on PBCH or on PSS/SSS and does not require additional FFT compared to the legacy UE. The number of FFT operations for the UE without CE using QSI will be n_{Sync} with probability pq when QSI is detected and indicates "sleep". Otherwise, the UE resumes legacy operation and number of FFT operations will be equal to n_{Legacy}. Therefore, the total number of FFT operations for the UE implementing QSI on PBCH or QSI on PSS/SSS is given by

$$n_{\text{QSI}} = pq n_{\text{Sync}} + (1 - pq) n_{\text{Legacy}}. \tag{11}$$

3) MTC UE with CE adopting our DRX with QSI mechanism: In this case, the QSI signal is transmitted on PDSCH. The UE buffers the entire QSI sub-frame and tries to detect the QSI signal. Since we transmit the QSI on 1 PRB in the PDSCH space, the minimum FFT size in LTE/LTE-A which is a 128 point FFT, is sufficient to obtain the QSI signal. Thus, the number of FFT operations for detecting the QSI signal can be calculated as $n_{\text{Q}} = 14 \times 128 \log_2(128) \times r_{\text{Q}} = 12544 r_{\text{Q}}$, where r_{Q} is the number of repetitions required to decode the QSI signal successfully. If the QSI signal is detected successfully and if it indicates "sleep", the number of FFT operations will be equal to n_{Q} which occurs with a probability pq. If the QSI signal is detected successfully and if it indicates "stay-awake", it will be $n_{\text{Q}} + n_{\text{PDCCH}} r_{\text{PDCCH}}$ which happens with probability $p(1-q)$. If the QSI is not detected, then the number of FFT operations will be $n_{\text{Q}} + n^{\text{CE}}_{\text{Legacy}}$. Therefore, the total number of FFT operations for UE with CE adopting QSI is

$$\begin{aligned} n^{\text{CE}}_{\text{QSI}} = {} & pq n_{\text{Q}} + p(1-q)(n_{\text{Q}} + n_{\text{PDCCH}} r_{\text{PDCCH}}) \\ & + (1-p)(n_{\text{Q}} + n^{\text{CE}}_{\text{Legacy}}). \end{aligned} \tag{12}$$

TABLE II
SIMULATION PARAMETERS

eNB Parameters	**Value**
Antenna Configuration	2Tx × 1Rx
Number of downlink RBs	6
Physical Hybrid-ARQ Indicator Channel (PHICH) duration	Normal
HICH Group Multiplier	$\frac{1}{6}$
System Frame Number	randi([0 255])
Cell ID	0
No. PDCCH symbols, m	2
UE Parameters	**Value**
Antenna Configuration	1Tx × 1Rx
VCO accuracy	10ppm
DRX cycle length, t_{DRX}	[1.28s, 2.56s, 10.24s, 1min, 10min]
Drift time, t_{Drift}	VCO accuracy × t_{DRX}
ON time for paging decode, t_{Paging}	1ms (normal coverage) 10ms (CE mode)
ON state power, P_{ON}	500mW
"Light Sleep" power, P_{LS}	250mW
"Deep Sleep" power, P_{DS}	0.0185mW
Probability of successful QSI detection, p	0.9
Probability that QSI indicates "sleep", q	0.9

VI. SIMULATION RESULTS AND ANALYSIS

In this section, we highlight the benefits of the proposed QSI solutions for LTE/LTE-A for IoT through simulation results and detailed analysis of the UE energy efficiency and computational complexity when our QSI mechanisms are used.

A. Simulation Results

The different QSI solutions introduced in this paper were simulated using the LTE system toolbox on MATLAB. The simulations were run for the Extended Pedestrian-A (EPA) channel model with a Doppler Spread of 1Hz and the number of QSI bits, $M = 4$. This channel model was selected since it is recommended by the 3GPP for testing low UE mobility [30] and is suitable for the IoT scenarios considered in this work such as pet tracking and weather sensing in the case of normal coverage or patient monitoring in case of enhanced coverage. Other simulation parameters are listed in Table II.

The QSI solutions for MTC UEs without CE discussed in Section III were analyzed using the block error rate (BLER) performance considering the minimum SNR required for 10% BLER ($S_{10\%}$) as the performance indicator. For MTC UEs with CE, we considered 15dB CE and obtained the operating SNR for the synchronization channel as -14.2dB [10]. We evaluated the performance based on the accumulation time required for 90% detection (t_{Acc}) of the desired signal (PSS/SSS for the legacy UE and the QSI signal for UE with QSI) for

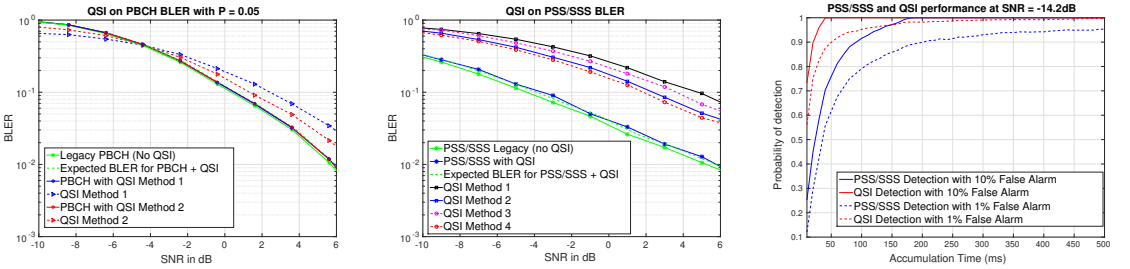

(a) QSI on PBCH (b) QSI on PSS/SSS (c) Re-Sync and QSI on PDSCH for CE

Fig. 4. Legacy and QSI performance results

TABLE III
PERFORMANCE SUMMARY USING $S_{10\%}$ (FOR UES WITHOUT CE) AND t_{Acc} (FOR UES WITH CE)

PBCH $S_{10\%}$ (No CE)	QSI on PBCH (No CE)	PSS/SSS $S_{10\%}$ (No CE)	QSI on PSS/SSS $S_{10\%}$ (No CE)	Legacy PSS/SSS t_{Acc} (15dB CE)	QSI on PDSCH t_{Acc} (15dB CE)
Legacy: 0.35dB With QSI: Met 1: 0.53dB Met 2: 0.55dB	Met 1: 2.43dB Met 2: 1.33dB	Legacy: -4.41dB With QSI: -3.62dB	Met 1: 4.79dB Met 2: 2.37dB Met 3: 3.62dB Met 4: 1.85dB	FA 10%: 90ms FA 1%: 200ms	FA 10%: 20ms FA 1%: 50ms

false alarm (FA) rates of 10% and 1%. Table III summarizes the performance results for the different QSI solutions.

The results for QSI on PBCH and QSI on PSS/SSS are shown in Fig. 4a and Fig. 4b respectively. From Table III, we note that the two QSI on PBCH solutions show 0.18dB and 0.2dB degradation in PBCH detection performance respectively for 10% BLER, which is close to the expected loss calculated as $10\log_{10}(1-P) = 0.22$dB with $P = 0.05$ in Section III. For the AWGN channel results in [28], the QSI signal using our proposed methods acted as interference to the PBCH signal and degraded the PBCH detection performance by more than 0.5dB. The same is true in the current simulation too, but the EPA channel is not a static channel like AWGN and the degradation in PBCH detection performance is not as pronounced as it was for AWGN. For QSI on PSS/SSS, the expected loss in PSS/SSS detection performance when QSI is transmitted on the unused sub-carriers is 0.54dB as computed in Section III. From Table III, we observe that the loss obtained from our simulation is 0.79dB for 10% BLER, which is close to our expected results.

We observe that for QSI on PBCH using spreading, repetition and (8,4) Extended Hamming Code (method 2) gives the best performance and for QSI on PSS/SSS, the method of transmitting QSI using the unused carriers of both PSS and SSS along with (8,4) Extended Hamming Code (method 4) gives the best performance. Comparing the $S_{10\%}$ for these two methods, we can see that QSI on PBCH (method 2) is 0.52dB better than QSI on PSS/SSS (method 4) owing to the SNR gain due to spreading.

In the case of MTC UEs with CE, we determined the number of PSS/SSS repetitions required to re-acquire the symbol timing when the UE wakes up for the legacy UE. Since we look at the case where the UE had already obtained the cell identifier before it went to sleep, the PSS/SSS is known to the UE. Therefore, the UE need not hypothesize over all combinations of PSS/SSS and has to re-acquire the same PSS/SSS combination which it detected before. Since the SSS and PSS are on consecutive symbols, we considered them as one long sequence and used differential auto-correlation to detect this long sequence and obtain the symbol boundary. A successful detection is registered when we detect the correct symbol boundary, otherwise it is regarded as a false alarm. Similarly, we obtained the QSI detection performance with the QSI transmitted on PDSCH. Fig. 4c indicates the re-sync performance of the legacy UE and the QSI detection performance for MTC UE with CE. Using the 15dB CE results summarized in Table III, we observe that for the legacy UE requires $t_{\mathrm{Acc}} = 200$ms (40 PSS/SSS repetitions), while the UE adopting our QSI on PDSCH mechanism requires $t_{\mathrm{Acc}} = 50$ms (20 QSI repetitions) at a false alarm rate of 1%. Therefore, the re-acquisition time of the UE is reduced by a factor of 4 at this false alarm rate when our QSI mechanism is adopted, which improves the energy efficiency.

B. Energy Efficiency Results

The energy efficiency is calculated as the ratio of the energy consumed by the UE using our QSI solution to the energy consumed by the legacy UE. The energy consumed by the legacy UE was computed using (2) and the energy consumed by the UE using QSI was computed using (4) or (8) depending on whether it is in normal coverage mode or coverage enhancement mode with the parameters listed in Table II. For QSI on PDSCH, we considered 15dB CE and used $t_{\mathrm{Q}} = 50$ms and $t_{\mathrm{Sync}}^{\mathrm{CE}} = 200$ms corresponding to t_{Acc} at a false alarm rate of 1%.

Table IV summarizes the reduction in energy consumption obtained by using QSI for different DRX cycle lengths. With the VCO drift of 10ppm, the UE would require to decode the PBCH if it sleeps more than 8.2 minutes. When PBCH

TABLE IV
REDUCTION IN ENERGY CONSUMPTION FOR UE WITH QSI

DRX length	QSI on PBCH (No CE)	QSI on PSS/SSS (No CE)	QSI on PDSCH (15dB CE)
1.28s	45.67%	51.74%	63.88%
2.56s	44.67%	50.61%	63.86%
10.24s	39.48%	44.73%	63.75%
1 min	22.52%	25.52%	63.05%
10 min	7.36%	7.36%	56.49%

TABLE V
FFT COMPUTATION REDUCTION FOR UE WITH QSI

eNB Bandwidth	FFT Size (No CE)	QSI on PBCH or PSS/SSS (No CE)	QSI on PDSCH (15dB CE)
1.4MHz	128	10.69%	65.15%
5MHz	512	36.21%	65.73%
10MHz	1024	53.02%	66.55%
20MHz	2048	66.88%	68.12%

decoding is not required, QSI on PSS/SSS is more energy efficient than QSI on PBCH for MTC UEs without CE. If PBCH decoding is required, the energy efficiency obtained by both the QSI mechanisms is equivalent. For MTC UEs with CE, QSI on PDSCH demonstrates considerable improvement in energy efficiency since the ON time of the UE is reduced significantly. The energy efficiency is obtained by the reduction in the ON time of the UE which depends on the SNR and not on the length of the DRX cycle. Therefore, at a given SNR, the ratio of ON time to the DRX cycle length decreases with increasing DRX cycle length which leads to a decrease in the energy efficiency.

C. Computational Complexity Results

The computational reduction is calculated as the ratio of the number of FFT computations consumed by the UE using our QSI solutions to that of the legacy UE. We obtained the number of FFT computations for the legacy UE using (9) for normal mode and (10) for coverage enhancement mode. For the UE using our QSI solutions, we obtained the numbers from (11) and (12) for normal mode and CE mode respectively. The number of repetitions, r_{Sync}, r_{Q} and r_{PDCCH}, were chosen corresponding to t_{Sync}, t_{QSI} and t_{Paging} respectively. The computational reduction obtained for different QSI solutions is summarized in Table V. The PDCCH FFT size is directly proportional to the eNB bandwidth while QSI FFT size is always 128 point. Therefore, the computational efficiency increases for higher eNB bandwidths. This is true even for the CE case. Additionally, since the QSI detection requires a lesser number of repetitions than legacy PSS/SSS detection, the computational efficiency obtained for the CE case is higher than that for the non-CE case.

It should be noted that along with the full scale FFT, PDCCH message block decoding also requires Viterbi decoding and hypothesizing over 44 different possible locations, which is computationally intensive, but the QSI either uses correlation with 2^M different sequences or uses simple despreading and repetition combining (plus ML decoding for 2^M sequences in case of FEC), which are simpler methods compared to PDCCH blind decoding. This leads to further improvement in computational savings. Such an analysis is not modeled in this paper and is being considered for future work.

VII. CONCLUSION

In this paper, we have considered the problem of improving the current DRX and paging mechanism for energy efficient IoT using LTE/LTE-A. We have proposed a modified DRX mechanism incorporating quick sleeping as a novel, simple and efficient solution for this problem. Our QSI solutions are in line with the current standardization activities for MTC in 3GPP LTE/LTE-A to facilitate IoT and have minimal influence on the legacy UEs. For the MTC UEs in normal coverage, we proposed QSI on PBCH and QSI on PSS/SSS mechanisms which do not require additional resources. For UEs with coverage enhancement, we introduced the QSI mechanism using dedicated resources on PDSCH. The different QSI solutions were simulated on the EPA-1Hz channel model to address the case of low-mobility. We also determined the reduction in energy consumption and computational complexity for the MTC UEs using our QSI mechanisms when compared to the legacy UEs. For MTC UEs without CE using our QSI solutions, we showed 45% and 66% reduction in energy consumption and computational complexity respectively. For MTC UEs with 15dB CE using QSI on PDSCH, we demonstrated that we could obtain 63% reduction in energy consumption and 68% reduction in computational complexity. The task of testing our solutions on other channel models such as vehicular channel and improving our computation complexity model constitutes our future work.

ACKNOWLEDGEMENTS

The authors would like to thank MITACS, Canada for supporting this work.

REFERENCES

[1] "IEEE Standard for Local and metropolitan area networks–Part 15.4: Low-Rate Wireless Personal Area Networks (LR-WPANs)," *IEEE Std 802.15.4-2011*, 2011.
[2] D. Raychaudhuri and N. B. Mandayam, "Frontiers of wireless and mobile communications," *Proc. of the IEEE*, vol. 100, no. 4, pp. 824–840, 2012.
[3] "IEEE Standard for Information technology–Telecommunications and information exchange between systems–Local and metropolitan area networks–Specific requirements–Part 11: Wireless LAN Medium Access Control (MAC) and Physical Layer (PHY) Specifications," *IEEE Std 802.11-2012*, 2012.
[4] S. Aust, R. V. Prasad, and I. G. Niemegeers, "IEEE 802.11 ah: Advantages in standards and further challenges for sub 1 GHz Wi-Fi," in *IEEE Int. Conf. on Commun.*, 2012, pp. 6885–6889.
[5] I. Hwang, B. Song, and S. S. Soliman, "A holistic view on hyper-dense heterogeneous and small cell networks," *IEEE Commun. Mag.*, vol. 51, no. 6, pp. 20–27, 2013.
[6] A. Damnjanovic, J. Montojo, Y. Wei, T. Ji, T. Luo, M. Vajapeyam, T. Yoo, O. Song, and D. Malladi, "A survey on 3GPP heterogeneous networks," *IEEE Wireless Commun. Mag.*, vol. 18, no. 3, pp. 10–21, 2011.

[7] J. Ramiro and K. Hamied, *Self-Organizing Networks (SON): Self-Planning, Self-Optimization and Self-Healing for GSM, UMTS and LTE*. John Wiley & Sons, 2011.
[8] M. Peng, D. Liang, Y. Wei, J. Li, and H.-H. Chen, "Self-configuration and self-optimization in LTE-Advanced heterogeneous networks," *IEEE Commun. Mag.*, vol. 51, no. 5, pp. 36–45, 2013.
[9] D. Astely, E. Dahlman, G. Fodor, S. Parkvall, and J. Sachs, "LTE release 12 and beyond," *IEEE Commun. Mag.*, vol. 51, no. 7, 2013.
[10] 3GPP, "Study on provision of low-cost Machine-Type Communications (MTC) User Equipments (UEs) based on LTE," 3GPP, TR 36.888, Jun. 2013.
[11] ——, "Study on Machine-Type Communications (MTC) and other mobile data applications communications enhancements," 3GPP, TR 23.887, Dec. 2013.
[12] X. Liang, X. Li, M. Barua, L. Chen, R. Lu, X. Shen, and H. Luo, "Enabling pervasive healthcare through continuous remote health monitoring," *IEEE Wireless Commun. Mag.*, vol. 19, no. 6, pp. 10–18, 2012.
[13] T. Taleb and A. Kunz, "Machine type communications in 3GPP networks: potential, challenges, and solutions," *IEEE Commun. Mag.*, vol. 50, no. 3, pp. 178–184, 2012.
[14] F. Ghavimi and H.-H. Chen, "M2M communications in 3GPP LTE/LTE-A networks: Architectures, service requirements, challenges, and applications," *IEEE Commun. Surveys Tuts.*, 2015.
[15] A. Rajandekar and B. Sikdar, "A survey of MAC layer issues and protocols for machine-to-machine communications," *IEEE Internet of Things Journal*, vol. 2, no. 2, pp. 175–186, 2015.
[16] C. S. Bontu and E. Illidge, "DRX mechanism for power saving in LTE," *IEEE Commun. Mag.*, vol. 47, no. 6, pp. 48–55, 2009.
[17] 3GPP, "Evolved Universal Terrestrial Radio Access (E-UTRA); Medium Access Control (MAC) protocol specification," 3GPP, TS 36.321, Mar. 2014.
[18] ——, "Evolved Universal Terrestrial Radio Access (E-UTRA); Physical layer procedures," 3rd Generation Partnership Project (3GPP), TS 36.213, Mar. 2014.
[19] ——, "Evolved Universal Terrestrial Radio Access (E-UTRA); User Equipment (UE) procedures in idle mode," 3GPP, TS 36.304, Mar. 2014.
[20] L. Zhou, H. Xu, H. Tian, Y. Gao, L. Du, and L. Chen, "Performance analysis of power saving mechanism with adjustable DRX cycles in 3GPP LTE," in *Proc. IEEE 68th Veh. Technol. Conf.-Fall*, 2008, pp. 1–5.
[21] S. Jin and D. Qiao, "Numerical analysis of the power saving in 3GPP LTE advanced wireless networks," *IEEE Trans. Veh. Technol.*, vol. 61, no. 4, pp. 1779–1785, 2012.
[22] K. Zhou, N. Nikaein, and T. Spyropoulos, "LTE/LTE-A discontinuous reception modeling for machine type communications," *IEEE Wireless Commun. Lett.*, vol. 2, no. 1, pp. 102–105, 2013.
[23] A. T. Koc, S. C. Jha, R. Vannithamby, and M. Torlak, "Device power saving and latency optimization in LTE-A networks through DRX configuration," *IEEE Trans. Wireless Commun.*, vol. 13, no. 5, pp. 2614–2625, 2014.
[24] C. Tseng, H. Wang, F. Kuo, K. Ting, H. Chen, and G. Chen, "Delay and power consumption in LTE/LTE-A DRX mechanism with mixed short and long cycles," *IEEE Trans. Veh. Technol.*, vol. PP, no. 99, pp. 1–1, 2015.
[25] T. Tirronen, A. Larmo, J. Sachs, B. Lindoff, and N. Wiberg, "Reducing energy consumption of LTE devices for machine-to-machine communication," in *Proc. IEEE Global Telecommun. Conf. Wkshps.*, 2012, pp. 1650–1656.
[26] S. Kim, K. Jung, J. Choi, and Y. Kwak, "Improving LTE/LTE-A UE power efficiency with extended DRX cycle," in *Proc. IEEE 80th Veh. Technol. Conf.-Fall*, 2014, pp. 1–5.
[27] S. C. Jha, A. T. Koc, and R. Vannithamby, "Device power saving mechanisms for low cost MTC over LTE networks," in *IEEE Int. Conf. on Commun. Wkshps.*, 2014, pp. 412–417.
[28] N. M. Balasubramanya, L. Lampe, G. Vos, and S. Bennett, "Introducing quick sleeping using the broadcast channel for 3GPP LTE MTC," in *Proc. IEEE Global Telecommun. Conf. Wkshps.*, 2014, pp. 606–611.
[29] H. Holma and A. Toskala, *LTE for UMTS: Evolution to LTE-Advanced*. John Wiley & Sons, 2011.
[30] 3GPP, "User Equipment (UE) Radio Transmission and Reception." 3GPP, TS 36.101, Mar. 2014.